CONTACT INTERACTION OF COMPOSITE SHELLS, SUBJECTED TO FOLLOWER LOADS, WITH A RIGID CONVEX FOUNDATION

G. M. Kulikov* and S. V. Plotnikova

Keywords: *multilayered composite shell, follower load, contact problem, tire, geometrically exact shell element, 7-parameter shell model*

Based on a 7-parameter shell model, a numerical algorithm is developed for solving the contact problem for a multilayered composite shell lying on a rigid convex foundation, which is subjected to a follower pressure and undergoes arbitrarily large rotations. A new geometrically exact solid shell element is formulated, which permits one to solve the nonlinear deformation problem for thin-walled composite structures under unilateral contact constraints by using a small number of load steps. The calculation of a homogeneous ring and an angle-ply toroidal shell interacting with plane and cylindrical foundations is considered.

Introduction

Based on the modified method of Lagrange polynomials with regularization [7], considerable progress has been made recently in solving geometrically nonlinear shell problems in the case of contact restrictions [1-6]. For example, in [1-3], isoparametric finite elements are used, while the studies [4-6] are dedicated to geometrically exact shell elements based on a 6-parameter model in which the deformation relations faithfully represent arbitrarily large rigid-body shell displacements in curvilinear coordinates of a reference surface. The term "geometrically exact shell element" means that the reference surface of the shell is described by analytically specified functions, and the displacement vectors of external surfaces are represented in a local basis related to the reference surface of the shell. The drawback of the 6-parameter model of multilayer shells is that the transverse normal strains in it are uniformly distributed across the thickness of layer package, which leads to the Poisson locking of shell elements, i.e., to an artificial overestimation of the rigidity of the shell element in the transverse direction. An alternative is the 7-parameter 3D shell model used in [8, 9], which is free from this drawback.

In the present study, based on the 7-parameter shell model, a new algorithm for numerically solving the geometrically nonlinear contact problems of multilayer composite shells under the action of a follower load is suggested. According to this algorithm, the value of the nodal contact force operating along the normal to the limiting surface is connected with the Lagrange multiplier λ in the form $\lambda|\text{grad}\,\Psi|$, where Ψ is the function of nonpenetration of contacting bodies. In this case, rather large loading steps can be employed, depending on the geometrically exact shell element [9]. We should note that, in [1-5], the Lagrange multiplier is assumed equal to the contact pressure for all nodes coming into contact with the rigid foundation, which is com-

---

Tambov State Technical University, Russia. Translated from Mekhanika Kompozitnykh Materialov, Vol. 45, No. 6, pp. 61-78, January-February, 2010. Original article submitted March 2, 2009.

*Corresponding author; e-mail: kulikov@apmath.tstu.ru.

0191-5665/10/4601-0043

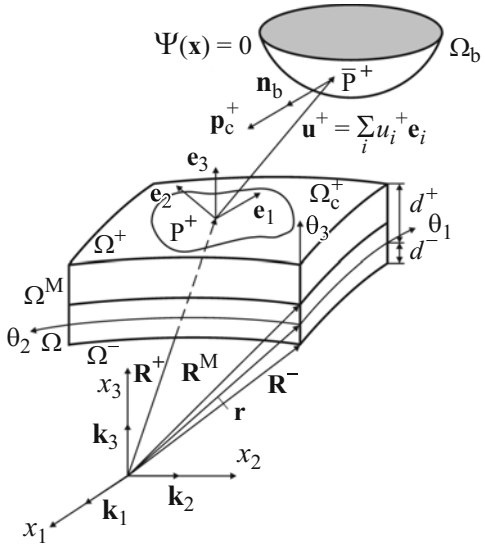

Fig. 1. Contact interaction of a shell with a rigid convex body.

monly accepted in the mechanics of contact interactions. However, this condition quite often leads to inefficient calculations in the cases of thin-walled structures subjected to large displacements and arbitrarily large rotations.

Formulation of the Contact Problem for a Composite Shell

Let us consider a thin shell of thickness $h = d^- + d^+$ composed of *NL* elastic anisotropic layers of constant thickness h_k. We assume that, at each point of the shell, there is a surface of elastic symmetry parallel to a reference surface Ω. As the reference surface, we take the inner surface of a *k*-layer or a layer interface and relate it to curvilinear orthogonal coordinates θ_1 and θ_2, reckoned along the lines of main curvatures. The transverse coordinate θ_3 is reckoned toward the increasing external normal to the surface Ω (Fig. 1). Let $\mathbf{e}_1$ and $\mathbf{e}_2$ be the unit vectors of tangents to the coordinate lines θ_1 and θ_2, $\mathbf{e}_3$ the unit vector of the external normal, A_α the Lamé parameters, k_α the main curvatures, d^{A} the distances from the reference to external surfaces Ω^{A}, $r(\theta_1, \theta_2)$ the radius vector of the reference surface Ω, $\mathbf{R}^{\mathrm{M}}(\theta_1, \theta_2)$ the radius vector of the midsurface Ω^{M}, and $\mathbf{R}^{\mathrm{A}}(\theta_1, \theta_2)$ the radii vectors of the external surfaces Ω^{A}. Hereinafter, $k = 1, 2, ..., NL$; $\alpha, \beta = 1, 2$; $i, j = 1, 2, 3$; $\mathrm{A} = -, +$.

For definiteness, we assume that the contact interaction of the shell is realized only with one absolutely rigid body, without account of friction in the contact area. Let the boundary of the motionless convex body Ω_{b} be sufficiently smooth and be described by the equation

$$\Psi(\mathbf{x}) = 0, \tag{1}$$

where $\mathbf{x} = \sum_i x_i \, \mathbf{k}_i$ is the radius vector of the surface Ω_{b}. For the set of points outside the rigid body, the inequality

$$\Psi(\mathbf{x}) > 0 \tag{2}$$

is valid.

Conditions (1) and (2) can be regarded as *nonpenetration condition*s for the shell and the rigid body. They express the fact that the two contacting bodies must remain in contact according to condition (1) or be separated according to inequality (2).

For simplicity, we assume that no contact interaction occurs on the lower surface Ω^-, but the surface Ω^+ consists of two parts: $\Omega^+ = \Omega_f^+ \cup \Omega_c^+$, where Ω_f^+ is the part with a given external surface load, and Ω_c^+ is the part where a contact interaction is expected. In this case, the *condition of nonnegative* contact pressure has the form

$$p_c^+ = -\mathbf{p}_c^+ \cdot \mathbf{n}_b \le 0, \tag{3}$$

where $\mathbf{n}_b$ is the unit vector of the external normal to the surface Ω_b (Fig. 1).

Conditions (1)-(3) can be written in the form of one equation

$$p_c^+(\mathbf{R}^+)\Psi(\overline{\mathbf{R}}^+) = 0, \tag{4}$$

with

$$\overline{\mathbf{R}}^+ = \mathbf{R}^+ + \mathbf{u}^+ = \sum_i \overline{R}_i^+ \mathbf{k}_i, \quad \overline{R}_i^+ = r_i + d^+ t_{3i} + \sum_j t_{ji} u_j^+, \tag{5}$$

where $r_i(\theta_1, \theta_2)$ are components of the radius vector of the reference surface; $u_i^+(\theta_1, \theta_2)$ are components of the displacement vector of the external surface; $t_{ij}(\theta_1, \theta_2)$ are elements of the matrix of transition from the basis $\mathbf{k}_i$ of Cartesian coordinates to the local basis $\mathbf{e}_i$; $\overline{R}_i^+(\theta_1, \theta_2)$ are components of the radius vector of the external surface of the deformed shell. Condition (4) means that the contact forces are determined only at the shell points where a contact interaction with the rigid foundation is realized.

To introduce contact restrictions (4) into a variational formulation of the problem, we consider the modified Hu–Washizu functional

$$J_{PL} = J_{HW} + \iint_{\Omega_c^+} \left[\lambda \Psi(\overline{\mathbf{R}}^+) - \frac{\lambda^2}{2\epsilon} \right] d\Omega, \tag{6}$$

where J_{HW} is the Hu–Washizu functional [4, 6]; $\lambda(\mathbf{R}^+)$ is the Lagrange multiplier; ϵ is a positive penalty parameter, which is introduced for regularization of the problem. In the case $\epsilon \to \infty$, we come to the standard formulation of the problem of contact interaction between a shell and a rigid foundation [3]. We should note that the functional J_{PL} is often called the perturbed Lagrangian [7].

The stationarity condition of functional (6) leads to the variational equation

$$\delta J_{HW} + \delta J_c = 0, \tag{7}$$

$$\delta J_c = \iint_{\Omega_c^+} \left\{ \lambda \delta \Psi(\overline{\mathbf{R}}^+) + \delta\lambda \left[\Psi(\overline{\mathbf{R}}^+) - \frac{1}{\epsilon}\lambda \right] \right\} d\Omega, \tag{8}$$

whence, with account of the results presented in [6], follows a fundamental formula relating the contact pressure with the Lagrange multiplier:

$$p_c^+ = \lambda(\mathbf{R}^+) \left| \operatorname{grad} \Psi(\overline{\mathbf{R}}^+) \right|. \tag{9}$$

The displacements and the components of the Green–Lagrange strain tensor of the 7-parameter model of multilayer shells [9] are distributed across the thickness of layer package according to the formulas

$$u_\alpha = \sum_A N^A u_\alpha^A, \quad u_3 = \sum_I L^I u_3^I \quad (I = -, M, +), \tag{10}$$

$$\varepsilon_{\alpha\beta} = \sum_{\mathrm{A}} N^{\mathrm{A}} \varepsilon^{\mathrm{A}}_{\alpha\beta}, \quad \varepsilon_{33} = \sum_{\mathrm{A}} N^{\mathrm{A}} \varepsilon^{\mathrm{A}}_{33}, \; \varepsilon_{\alpha 3} = \widehat{\varepsilon}_{\alpha 3}, \quad \widehat{\varepsilon}_{\alpha 3} = \frac{1}{2}(\varepsilon^{-}_{\alpha 3} + \varepsilon^{+}_{\alpha 3}), \tag{11}$$

where $u_i^{\mathrm{A}}(\theta_1, \theta_2)$ are the tangential and transverse displacements of external surfaces; $u_3^{\mathrm{M}}(\theta_1, \theta_2)$ is the transverse displacement of the midsurface; $\varepsilon_{ij}^{\mathrm{A}}(\theta_1, \theta_2)$ are the strains of external surfaces [9]; $N^{\mathrm{A}}(\theta_3)$ and $L^I(\theta_3)$ are the Lagrange polynomials of the first and second degrees, respectively. It should be noted that deformation relations (11) exactly represent arbitrarily large rigid-body displacements of the shell and allow us to overcome the Poisson locking of shell elements in the transverse direction [8].

Geometrically Exact Hybrid Bilinear Element of a Composite Shell in the Presence of Unilateral Restrictions

In [9], a geometrically exact 7-parameter bilinear element of a composite shell subjected to the action of a follower load has been constructed, which is based on the displacement-independent strains

$$\varepsilon^{\mathrm{AS}}_{\alpha\beta} = \sum_{\mathrm{A}} N^{\mathrm{A}} E^{\mathrm{A}}_{\alpha\beta}, \quad \varepsilon^{\mathrm{AS}}_{33} = \sum_{\mathrm{A}} N^{\mathrm{A}} E^{\mathrm{A}}_{33}, \quad \varepsilon^{\mathrm{AS}}_{\alpha 3} = E_{\alpha 3}, \tag{12}$$

where $E^{\mathrm{A}}_{\alpha\beta}(\theta_1, \theta_2)$, $E^{\mathrm{A}}_{33}(\theta_1, \theta_2)$, and $E_{\alpha 3}(\theta_1, \theta_2)$ are independently introduced strains of external surfaces of the shell. As is seen, the distribution laws of displacement-independent strains (11) and (12) agree with each other.

It is known that functional variables of different types are introduced in constructing a hybrid shell element, therefore, independent approximations must be used for them on each finite element. For displacements, we can employ the standard bilinear approximation

$$\mathbf{v} = \sum_r N_r \mathbf{v}_r,$$
$$\mathbf{v} = [u_1^- \; u_2^- \; u_3^- \; u_1^+ \; u_2^+ \; u_3^+ \; u_3^{\mathrm{M}}]^{\mathrm{T}}, \quad \mathbf{v}_r = [u_{1r}^- \; u_{2r}^- \; u_{3r}^- \; u_{1r}^+ \; u_{2r}^+ \; u_{3r}^+ \; u_{3r}^{\mathrm{M}}]^{\mathrm{T}}, \tag{13}$$

where $\mathbf{v}_r$ are the columns of nodal displacements; $N_r(\xi_1, \xi_2)$ are bilinear shape functions; $\xi_\alpha = (\theta_\alpha - d_\alpha^{\mathrm{el}})/l_\alpha^{\mathrm{el}}$ are normalized curvilinear coordinates of the element; d_α^{el} are center coordinates of the element; $2l_\alpha^{\mathrm{el}}$ are the lengths of element sides. Hereinafter, $r = \overline{1, 4}$.

For the independently introduced strains (12), we have even simpler approximations:

$$\mathbf{E} = \sum_{r_1, r_2} (\xi_1)^{r_1} (\xi_2)^{r_2} \mathbf{Q}^{r_1 r_2} \mathbf{E}^{r_1 r_2},$$

$$\mathbf{E} = [E_{11}^- \; E_{11}^+ \; E_{22}^- \; E_{22}^+ \; E_{33}^- \; E_{33}^+ \; 2E_{12}^- \; 2E_{12}^+ \; 2E_{13} \; 2E_{23}]^{\mathrm{T}},$$

$$\mathbf{E}^{00} = [E_{11}^{-00} \; E_{11}^{+00} \; E_{22}^{-00} \; E_{22}^{+00} \; E_{33}^{-00} \; E_{33}^{+00} \; 2E_{12}^{-00} \; 2E_{12}^{+00} \; 2E_{13}^{00} \; 2E_{23}^{00}]^{\mathrm{T}}, \tag{14}$$

$$\mathbf{E}^{01} = [E_{11}^{-01} \; E_{11}^{+01} \; E_{33}^{-01} \; E_{33}^{+01} \; 2E_{13}^{01}]^{\mathrm{T}},$$

$$\mathbf{E}^{10} = [E_{22}^{-10} \; E_{22}^{+10} \; E_{33}^{-10} \; E_{33}^{+10} \; 2E_{23}^{10}]^{\mathrm{T}}, \quad \mathbf{E}^{11} = [E_{33}^{-11} \; E_{33}^{+11}]^{\mathrm{T}},$$

where $\mathbf{E}^{r_1 r_2}$ are columns constant inside the element, $\mathbf{Q}^{00}$ is the 10×10 unit matrix; $\mathbf{Q}^{01}$ and $\mathbf{Q}^{10}$ are 10×5 matrices, and $\mathbf{Q}^{11}$ is a 10×2 matrix, all introduced in [9] for a more compact representation of the resolving matrix equations. Hereinafter, $r_1, r_2 = 0$, 1. For the resulting stresses [9], we assume a similar approximation:

$$\mathbf{H} = \sum_{r_1, r_2} (\xi_1)^{r_1} (\xi_2)^{r_2} \mathbf{Q}^{r_1 r_2} \mathbf{H}^{r_1 r_2},$$

$$\mathbf{H} = [H_{11}^{-} \; H_{11}^{+} \; H_{22}^{-} \; H_{22}^{+} \; H_{33}^{-} \; H_{33}^{+} \; H_{12}^{-} \; H_{12}^{+} \; H_{13} \; H_{23}]^{\mathrm{T}},$$

$$\mathbf{H}^{00} = [H_{11}^{-00} \; H_{11}^{+00} \; H_{22}^{-00} \; H_{22}^{+00} \; H_{33}^{-00} \; H_{33}^{+00} \; H_{12}^{-00} \; H_{12}^{+00} \; H_{13}^{00} \; H_{23}^{00}]^{\mathrm{T}}, \tag{15}$$

$$\mathbf{H}^{01} = [H_{11}^{-01} \; H_{11}^{+01} \; H_{33}^{-01} \; H_{33}^{+01} \; H_{13}^{01}]^{\mathrm{T}},$$

$$\mathbf{H}^{10} = [H_{22}^{-10} \; H_{22}^{+10} \; H_{33}^{-10} \; H_{33}^{+10} \; H_{23}^{10}]^{\mathrm{T}}, \quad \mathbf{H}^{11} = [H_{33}^{-11} \; H_{33}^{+11}]^{\mathrm{T}},$$

where $\mathbf{H}^{r_1 r_2}$ are columns constant inside the element.

Since the formulas for components of the Green–Lagrange strain tensor retain all small members {see Eqs. (6) and (7) in [9]}, the strains of the external shell surfaces vary according to the square law inside the finite element

$$\boldsymbol{\varepsilon} = \sum_{s_1, s_2} (\xi_1)^{s_1} (\xi_2)^{s_2} \boldsymbol{\varepsilon}^{s_1 s_2},$$

$$\boldsymbol{\varepsilon}^{s_1 s_2} = (\mathbf{B}^{s_1 s_2} + \mathbf{A}^{s_1 s_2} \mathbf{V}) \mathbf{V}, \quad \mathbf{B}^{s_1 s_2} = \mathbf{0} \text{ at } s_1 = 2 \text{ or } s_2 = 2,$$

$$\boldsymbol{\varepsilon} = [\varepsilon_{11}^{-} \; \varepsilon_{11}^{+} \; \varepsilon_{22}^{-} \; \varepsilon_{22}^{+} \; \varepsilon_{33}^{-} \; \varepsilon_{33}^{+} \; 2\varepsilon_{12}^{-} \; 2\varepsilon_{12}^{+} \; 2\hat{\varepsilon}_{13} \; 2\hat{\varepsilon}_{23}]^{\mathrm{T}}, \tag{16}$$

$$\boldsymbol{\varepsilon}^{s_1 s_2} = [\varepsilon_{11}^{-s_1 s_2} \; \varepsilon_{11}^{+s_1 s_2} \; \varepsilon_{22}^{-s_1 s_2} \; \varepsilon_{22}^{+s_1 s_2} \; \varepsilon_{33}^{-s_1 s_2} \; \varepsilon_{33}^{+s_1 s_2} \; 2\varepsilon_{12}^{-s_1 s_2} \; 2\varepsilon_{12}^{+s_1 s_2} \; 2\hat{\varepsilon}_{13}^{s_1 s_2} \; 2\hat{\varepsilon}_{23}^{s_1 s_2}]^{\mathrm{T}}.$$

Here, $\mathbf{V} = [\mathbf{v}_1^{\mathrm{T}} \; \mathbf{v}_2^{\mathrm{T}} \; \mathbf{v}_3^{\mathrm{T}} \; \mathbf{v}_4^{\mathrm{T}}]^{\mathrm{T}}$ is the column of nodal displacements of an element of dimensions 28×1; $\mathbf{B}^{s_1 s_2}$ are 10×28 matrices, constant inside the element, corresponding to the account of linear components of the Green–Lagrange strain tensor; $\mathbf{A}^{s_1 s_2}$ are three-dimensional $10 \times 28 \times 28$ arrays, constant inside the element, corresponding to the account of nonlinear components of the Green–Lagrange strain tensor. In this case, $\mathbf{A}^{s_1 s_2} \mathbf{V}$ is a 10×28 matrix, where $s_1, s_2 = 0, 1, 2$.

In the case of sparse finite-element meshes, the characteristics of the geometrically exact bilinear shell element can be improved by applying the assumed natural strain (ANS) technique, which recently has been widely used in the literature on the finite-element method [10, 11]. We should note that, in the present study, the ANS method is employed in a nonconventional formulation, since it is assumed that the strains of external shell surfaces vary inside the element not by square law (16), but by the bilinear law

$$\boldsymbol{\varepsilon}^{\mathrm{ANS}} = \sum_{r} N_r \boldsymbol{\varepsilon}(\mathrm{P}_r), \tag{17}$$

where P_r are nodes of the element. Approximation (17) can conveniently be presented in the form

$$\boldsymbol{\varepsilon}^{\mathrm{ANS}} = \boldsymbol{\varepsilon}^{00} + \boldsymbol{\varepsilon}^{02} + \boldsymbol{\varepsilon}^{20} + \boldsymbol{\varepsilon}^{22} + \xi_1 (\boldsymbol{\varepsilon}^{10} + \boldsymbol{\varepsilon}^{12}) + \xi_2 (\boldsymbol{\varepsilon}^{01} + \boldsymbol{\varepsilon}^{21}) + \xi_1 \xi_2 \boldsymbol{\varepsilon}^{11}. \tag{18}$$

Integral (8) is calculated by using the bilinear approximation for the subintegral function. After integration with respect to the variables ξ_1 and ξ_2, we come to the formula

$$\delta J_{\mathrm{c}} = \sum_{r} \mu_r^{+} \left[\delta \mathbf{v}_r^{\mathrm{T}} \lambda_r \mathbf{\Phi}_r + \delta \lambda_r \left(\Psi_r - \frac{1}{\epsilon} \lambda_r \right) \right], \tag{19}$$

where

$$\mathbf{\Phi}_r = \left[0\,0\,0 \frac{\partial \Psi_r}{\partial u_{1r}^{+}} \cdot \frac{\partial \Psi_r}{\partial u_{2r}^{+}} \cdot \frac{\partial \Psi_r}{\partial u_{3r}^{+}} 0 \right]^{\mathrm{T}}, \tag{20}$$

$$\Psi_r = \Psi(\mathrm{P}_r), \quad \frac{\partial \Psi_r}{\partial u_{ir}^{+}} = \frac{\partial \Psi_r}{\partial u_i^{+}}(\mathrm{P}_r), \quad \mu^{+} = A_{1r}^{+} A_{2r}^{+} l_1^{\mathrm{el}} l_2^{\mathrm{el}}.$$

Here, $A_\alpha^{+} = A_\alpha (1 + k_\alpha d^{+})$ are the Lamé parameters of the external surface Ω^{+}. This scheme allows us to exclude the nodal values of the Lagrange multiplier λ_r at the element level. It should be noted that, in [4, 5], unlike the approach suggested, the Lagrange multiplier is approximated inside the element according to the bilinear law. As a result, the nodal values of Lagrange multiplier λ_r are not excluded at the element level, and, in the calculations, it is necessary to solve a system of linear algebraic equations whose number varies during the iterative solution of the problem.

Introducing the distributions of displacements and strains across the shell thickness, (10)-(12), and the finite-element approximations (13)-(15) and (18) into the mixed variational equation (7) and taking into account Eq. (19), we come to the equilibrium equations of the element

$$\mathbf{E}^{r_1 r_2} = (\mathbf{Q}^{r_1 r_2})^{\mathrm{T}} (\mathbf{B}^{r_1 r_2} + \mathbf{R}^{r_1 r_2} \mathbf{V}) \mathbf{V}, \quad \mathbf{H}^{r_1 r_2} = (\mathbf{Q}^{r_1 r_2})^{\mathrm{T}} \mathbf{D} \mathbf{Q}^{r_1 r_2} \mathbf{E}^{r_1 r_2},$$

$$\sum_{r_1, r_2} \frac{1}{3^{r_1 + r_2}} (\mathbf{B}^{r_1 r_2} + 2\mathbf{R}^{r_1 r_2} \mathbf{V})^{\mathrm{T}} \mathbf{Q}^{r_1 r_2} \mathbf{H}^{r_1 r_2} + \Xi \mathbf{\Lambda} = \mathbf{F} + p^{-} \mathbf{G}^{-}(\mathbf{V}). \tag{21}$$

Here, $\mathbf{\Lambda} = [\lambda_1\ \lambda_2\ \lambda_3\ \lambda_4]^{\mathrm{T}}$ is the column of nodal values of the Lagrange polynomial; $\mathbf{F}$ is a 28×1 column describing the action of a conservative load; p^{-} is a follower pressure distributed over the inner surface Ω^{-}; $\mathbf{G}^{-}(\mathbf{V})$ is a 28×1 column depending on the nodal displacements u_{ir}^{-} [9]; $\mathbf{D}$ is the matrix of elastic coefficients of the layered composite [9]; $\mathbf{R}^{r_1 r_2}$ are three-dimensional $10 \times 28 \times 28$ arrays; Ξ is a 28×4 matrix describing the contact interaction between the shell and rigid base:

$$\mathbf{R}^{00} = \mathbf{A}^{00} + \mathbf{A}^{02} + \mathbf{A}^{20} + \mathbf{A}^{22}, \quad \mathbf{R}^{01} = \mathbf{A}^{01} + \mathbf{A}^{21},$$

$$\mathbf{R}^{10} = \mathbf{A}^{10} + \mathbf{A}^{12}, \quad \mathbf{R}^{11} = \mathbf{A}^{11}, \tag{22}$$

$$\Xi = \frac{1}{4} \begin{bmatrix} \mathbf{\Phi}_1 & \mathbf{O}_{7\times1} & \mathbf{O}_{7\times1} & \mathbf{O}_{7\times1} \\ \mathbf{O}_{7\times1} & \mathbf{\Phi}_2 & \mathbf{O}_{7\times1} & \mathbf{O}_{7\times1} \\ \mathbf{O}_{7\times1} & \mathbf{O}_{7\times1} & \mathbf{\Phi}_3 & \mathbf{O}_{7\times1} \\ \mathbf{O}_{7\times1} & \mathbf{O}_{7\times1} & \mathbf{O}_{7\times1} & \mathbf{\Phi}_4 \end{bmatrix},$$

where $\mathbf{O}_{7\times1}$ is a 7×1 zero column.

Note 1. The system of equations (21), (22) was derived on the assumption that the metrics of the external shell surfaces are equivalent to the metrics of the midsurface Ω^{M}. At the same time, this assumption is not used when considering the integral δJ_{c} entering into variational equation (7), since this can lead to some errors upon formulation of contact restrictions for shells of moderate thickness. We should note that an analytical integration [8, 9] was also used, which is obviously the prerogative of a geometrically exact shell element.

Let us complement equilibrium equations (21) for the element by the contact conditions

$$\Psi_r = \frac{1}{\epsilon}\lambda_r, \quad \lambda_r \le 0 \quad \text{for} \quad r \in I_c,$$
$$\Psi_r > 0, \quad \lambda_r = 0 \quad \text{for} \quad r \notin I_c, \tag{23}$$

where $I_c \subset \{1,2,3,4\}$ is the set of element nodes coming into contact with the rigid body.

The nonlinear system (21) with restrictions (23) can be solved by using an incremental approach. Let us consider two deformed states (not necessarily close to each other) of the shell and mark the quantities describing the preceding state of the shell with a left superscript t and those belonging to the subsequent state with a left superscript $t+\Delta t$, i.e.,

$$^{t+\Delta t}p^- = {}^t p^- + \Delta p^-, \quad ^{t+\Delta t}\mathbf{V} = {}^t\mathbf{V} + \Delta\mathbf{V}, \quad ^{t+\Delta t}\mathbf{F} = {}^t\mathbf{F} + \Delta\mathbf{F}, \quad ^{t+\Delta t}\mathbf{\Lambda} = {}^t\mathbf{\Lambda} + \Delta\mathbf{\Lambda},$$
$$^{t+\Delta t}\mathbf{E}^{r_1r_2} = {}^t\mathbf{E}^{r_1r_2} + \Delta\mathbf{E}^{r_1r_2}, \quad ^{t+\Delta t}\mathbf{H}^{r_1r_2} = {}^t\mathbf{H}^{r_1r_2} + \Delta\mathbf{H}^{r_1r_2}, \tag{24}$$

where Δp^-, $\Delta\mathbf{V}$, $\Delta\mathbf{F}$, $\Delta\mathbf{\Lambda}$, $\Delta\mathbf{E}^{r_1r_2}$, and $\Delta\mathbf{H}^{r_1r_2}$ are incremental variables.

Inserting Eqs. (22) into Eqs. (20) and assuming that the latter are valid for an "instant of time" t, we come to an incremental form of equilibrium equations for the finite element of the shell in the presence of unilateral contact restrictions:

$$\Delta\mathbf{E}^{r_1r_2} = (\mathbf{Q}^{r_1r_2})^{\mathrm{T}}\,({}^t\mathbf{M}^{r_1r_2} + \mathbf{R}^{r_1r_2}\Delta\mathbf{V})\Delta\mathbf{V}, \tag{25}$$

$$\Delta\mathbf{H}^{r_1r_2} = (\mathbf{Q}^{r_1r_2})^{\mathrm{T}}\,\mathbf{D}\mathbf{Q}^{r_1r_2}\Delta\mathbf{E}^{r_1r_2}, \tag{26}$$

$$\sum_{r_1,r_2}\frac{1}{3^{r_1+r_2}}[2(\mathbf{R}^{r_1r_2}\Delta\mathbf{V})^{\mathrm{T}}\mathbf{Q}^{r_1r_2}\,{}^t\mathbf{H}^{r_1r_2} + ({}^t\mathbf{M}^{r_1r_2} + 2\mathbf{R}^{r_1r_2}\Delta\mathbf{V})^{\mathrm{T}}\mathbf{Q}^{r_1r_2}\Delta\mathbf{H}^{r_1r_2}]$$
$$+ \Xi(^{t+\Delta t}\mathbf{V})^{t+\Delta t}\mathbf{\Lambda} - \Xi({}^t\mathbf{V})^t\mathbf{\Lambda} = \Delta\mathbf{F} + {}^{t+\Delta t}p^-\mathbf{G}^-(^{t+\Delta t}\mathbf{V}) - {}^t p^-\mathbf{G}^-({}^t\mathbf{V}),$$
$$^t\mathbf{M}^{r_1r_2} = \mathbf{B}^{r_1r_2} + 2\mathbf{R}^{r_1r_2}\,{}^t\mathbf{V}. \tag{27}$$

Contact conditions (23) for the shell and rigid foundation are also presented in an incremental form:

$$\Psi_r(^{t+\Delta t}\mathbf{V}) = \frac{1}{\epsilon}{}^{t+\Delta t}\lambda_r, \quad ^{t+\Delta t}\lambda_r \le 0 \quad \text{for} \quad r \in {}^{t+\Delta t}I_c,$$
$$\Psi_r(^{t+\Delta t}\mathbf{V}) > 0, \quad ^{t+\Delta t}\lambda_r = 0 \quad \text{for} \quad r \notin {}^{t+\Delta t}I_c, \tag{28}$$

where $^{t+\Delta t}I_c \subset \{1,2,3,4\}$ is the set of nodes coming into contact at an "instant of time" $t+\Delta t$.

Excluding, with the help of Eqs. (28), the nodal values of Lagrange multiplier from Eq. (27), we obtain

$$\sum_{r_1,r_2}\frac{1}{3^{r_1+r_2}}[2(\mathbf{R}^{r_1r_2}\Delta\mathbf{V})^{\mathrm{T}}\mathbf{Q}^{r_1r_2}\,{}^t\mathbf{H}^{r_1r_2} + ({}^t\mathbf{M}^{r_1r_2} + 2\mathbf{R}^{r_1r_2}\Delta\mathbf{V})^{\mathrm{T}}\mathbf{Q}^{r_1r_2}\Delta\mathbf{H}^{r_1r_2}]$$
$$+ \epsilon(\Xi\Pi)(^{t+\Delta t}\mathbf{V}) - {}^{t+\Delta t}p^-\mathbf{G}^-(^{t+\Delta t}\mathbf{V}) = \Delta\mathbf{F} + \Xi({}^t\mathbf{V})\,{}^t\mathbf{\Lambda} - {}^t p^-\mathbf{G}^-({}^t\mathbf{V}), \tag{29}$$

where

$$\mathbf{\Pi} = [\Pi_1\ \Pi_2\ \Pi_3\ \Pi_4]^{\mathrm{T}}, \quad \Pi_r = \begin{cases}\Psi_r & \text{for} \quad r \in {}^{t+\Delta t}I_c,\\ 0 & \text{for} \quad r \notin {}^{t+\Delta t}I_c.\end{cases}$$

Incremental equations (25), (26), and (29) can be solved by the Newton–Raphson method, presenting the iteration process in the form

$$\Delta\mathbf{V}^{[n+1]} = \Delta\mathbf{V}^{[n]} + \Delta\hat{\mathbf{V}}^{[n]}, \quad \Delta\mathbf{E}^{r_1r_2[n+1]} = \Delta\mathbf{E}^{r_1r_2[n]} + \Delta\hat{\mathbf{E}}^{r_1r_2[n]},$$
$$\Delta\mathbf{H}^{r_1r_2[n+1]} = \Delta\mathbf{H}^{r_1r_2[n]} + \Delta\hat{\mathbf{H}}^{r_1r_2[n]} \quad (n = 0, 1,...). \tag{30}$$

Substituting relations (30) into Eqs. (25), (26), and (29), linearizing the resulting equations, and excluding the incremental strains $\Delta\hat{\mathbf{E}}^{r_1r_2[n]}$ and the incremental resulting strains $\Delta\hat{\mathbf{H}}^{r_1r_2[n]}$, we come to the resolving FEM system of equations

$$\mathbf{K}\Delta\hat{\mathbf{V}}^{[n]} = \Delta\boldsymbol{F}^{[n]}. \tag{31}$$

Here, $\mathbf{K} = \mathbf{K}_\mathrm{D} + \mathbf{K}_\mathrm{H} + \mathbf{K}_\mathrm{L} + \in \mathbf{K}_\mathrm{C}$ is the tangential rigidity matrix of the shell element and $\Delta\boldsymbol{F}^{[n]}$ is the column of right-hand sides, which are calculated from the formulas

$$\mathbf{K}_\mathrm{D} = \sum_{r_1,r_2} \frac{1}{3^{r_1+r_2}} ({}^t\mathbf{L}^{r_1r_2[n]})^\mathrm{T}\, \mathbf{D}^{r_1r_2}\, {}^t\mathbf{L}^{r_1r_2[n]},$$

$$\mathbf{K}_\mathrm{H} = 2\sum_{r_1,r_2} \frac{1}{3^{r_1+r_2}} (\mathbf{Q}^{r_1r_2}\, {}^t\mathbf{H}^{r_1r_2} + \mathbf{Q}^{r_1r_2}\Delta\mathbf{H}^{r_1r_2[n]})\mathbf{R}^{r_1r_2},$$

$$\mathbf{K}_\mathrm{L} = -({}^tp^- + \Delta p^-)\frac{\partial\mathbf{G}^-}{\partial\mathbf{V}}({}^t\mathbf{V} + \Delta\mathbf{V}^{[n]}),$$

$$\mathbf{K}_\mathrm{C} = \begin{bmatrix} \boldsymbol{\kappa}_1 & \mathbf{O}_{7\times7} & \mathbf{O}_{7\times7} & \mathbf{O}_{7\times7} \\ \mathbf{O}_{7\times7} & \boldsymbol{\kappa}_2 & \mathbf{O}_{7\times7} & \mathbf{O}_{7\times7} \\ \mathbf{O}_{7\times7} & \mathbf{O}_{7\times7} & \boldsymbol{\kappa}_3 & \mathbf{O}_{7\times7} \\ \mathbf{O}_{7\times7} & \mathbf{O}_{7\times7} & \mathbf{O}_{7\times7} & \boldsymbol{\kappa}_4 \end{bmatrix},$$

$$\Delta\boldsymbol{F}^{[n]} = \Delta\mathbf{F} - \sum_{r_1,r_2} \frac{1}{3^{r_1+r_2}} [({}^t\mathbf{L}^{r_1r_2[n]})^\mathrm{T}\, \mathbf{D}^{r_1r_2}\, ({}^t\mathbf{L}^{r_1r_2[n]} - \mathbf{R}^{r_1r_2}\Delta\mathbf{V}^{[n]})$$
$$+ 2(\mathbf{Q}^{r_1r_2}\, {}^t\mathbf{H}^{r_1r_2})\mathbf{R}^{r_1r_2}]\Delta\mathbf{V}^{[n]} - \in(\Xi\Pi)({}^t\mathbf{V} + \Delta\mathbf{V}^{[n]}) + \Xi({}^t\mathbf{V})\,{}^t\boldsymbol{\Lambda}$$
$$+ ({}^tp^- + \Delta p^-)\mathbf{G}^-({}^t\mathbf{V} + \Delta\mathbf{V}^{[n]}) - {}^tp^-\mathbf{G}^-({}^t\mathbf{V}),$$
$${}^t\mathbf{L}^{r_1r_2[n]} = \mathbf{B}^{r_1r_2} + 2\mathbf{R}^{r_1r_2}({}^t\mathbf{V} + \Delta\mathbf{V}^{[n]}), \quad \mathbf{D}^{r_1r_2} = \mathbf{Q}^{r_1r_2}(\mathbf{Q}^{r_1r_2})^\mathrm{T}\,\mathbf{D}\mathbf{Q}^{r_1r_2}(\mathbf{Q}^{r_1r_2})^\mathrm{T}, \tag{32}$$

where $\mathbf{O}_{7\times7}$ is a 7×7 zero matrix; $\boldsymbol{\kappa}_r$ are 7×7 matrices describing the contact interaction between the shell element nodes and the rigid foundation; $\boldsymbol{\kappa}_r = \mathbf{O}_{7\times7}$ for $r \notin {}^{t+\Delta t}I_\mathrm{c}$; for $r \in {}^{t+\Delta t}I_\mathrm{c}$, the nonzero elements of the corresponding matrices $\boldsymbol{\kappa}_r$ have the form

$$(\boldsymbol{\kappa}_r)_{3+i,3+j} = \left(\Psi_r \frac{\partial^2\Psi_r}{\partial u_{ir}^+ \partial u_{jr}^+} + \frac{\partial\Psi_r}{\partial u_{ir}^+}\cdot\frac{\partial\Psi_r}{\partial u_{jr}^+}\right)({}^t\mathbf{V} + \Delta\mathbf{V}^{[n]}). \tag{33}$$

The incremental resulting stresses at an nth step of the iterative process are calculated by the formula

$$\mathbf{Q}^{r_1r_2}\Delta\mathbf{H}^{r_1r_2[n]} = \mathbf{D}^{r_1r_2}[({}^t\mathbf{M}^{r_1r_2} + 2\mathbf{R}^{r_1r_2}\Delta\mathbf{V}^{[n-1]})\Delta\mathbf{V}^{[n]} - (\mathbf{R}^{r_1r_2}\Delta\mathbf{V}^{[n-1]})\Delta\mathbf{V}^{[n-1]}],$$

$$\Delta \mathbf{V}^{[0]} = \mathbf{0}, \quad \Delta \mathbf{H}^{r_1 r_2 [0]} = \mathbf{0}, \quad n = 1, 2, \ldots .$$

Further, employing the standard procedure of assembling shell elements, we derive the resolving system of linear equations in the global vector of incremental displacements $\Delta \mathbf{U}$. This system is solved, as in [9], by the modified Gauss method for banded matrices. The iterative process is continued until the fulfillment of the inequality

$$\left\| \Delta \mathbf{U}^{[n+1]} - \Delta \mathbf{U}^{[n]} \right\| < \varepsilon \left\| \Delta \mathbf{U}^{[n]} \right\|, \tag{34}$$

where $\|\ldots\|$ is the Euclidean norm in the space of displacements, and ε is the calculation accuracy required, which is specified a priori.

Note 2. It is obvious that the nonlinearity caused by the contact interaction between the shell and rigid body arises already in the process of finite-element discretization. It is the consequence of the fact that the set of nodes coming into contact, ${}^{t+\Delta t}I_{\mathrm{c}}^{\mathrm{A}} \subset \{1, 2, \ldots, N^{\mathrm{A}}\}$, is not known beforehand. To solve the problem, we use the trial-and-error method [3]. We assume that all the nodes already in contact are known at an "instant of time" $t + \Delta t$. Then the solution to the resolving system of equations can be found iteratively, by satisfying convergence criterion (34). The next stage consists in verification of the inequalities

$$\Psi_L ({}^{t+\Delta t}\mathbf{U}) > 0 \quad \text{for} \quad L \in {}^{t+\Delta t}I_{\mathrm{c}}^{\mathrm{A}}, \tag{35}$$

$$\Psi_L ({}^{t+\Delta t}\mathbf{U}) \le 0 \quad \text{for} \quad L \notin {}^{t+\Delta t}I_{\mathrm{c}}^{\mathrm{A}}. \tag{36}$$

If inequality (35) is fulfilled, the node is erroneous and is excluded from the contact zone. If inequality (36) is satisfied, the node is included into the set ${}^{t+\Delta t}I_{\mathrm{c}}^{\mathrm{A}}$. The process described proceeds until a correct solution is obtained.

Numerical Results

As a first example, we will consider the problem of contact interaction of a homogeneous ring, subjected to the action of a concentrated force P and a follower pressure p_0, with absolutely rigid plane and cylindrical ($R_{\mathrm{b}} = 100$ and $R_{\mathrm{b}} = 1000$) foundations. The geometrical and mechanical parameters of the ring are shown in Fig. 2a. The nonpenetration conditions for the contacting bodies, (1) and (2), can be presented by the relations

$$\Psi = \overline{R}_3^{+} \ge 0,$$

$$\overline{R}_3^{+} = \left(R + \frac{1}{2} h \right)(1 - \cos\varphi) + u_1^{+} \sin\varphi - u_3^{+} \cos\varphi$$

and

$$\Psi = \frac{1}{2R_{\mathrm{b}}} (\overline{R}_1^{+})^2 + \frac{1}{2R_{\mathrm{b}}} (\overline{R}_3^{+} + R_{\mathrm{b}})^2 - \frac{1}{2} R_{\mathrm{b}} \ge 0,$$

$$\overline{R}_1^{+} = \left(R + \frac{1}{2} h \right) \sin\varphi + u_1^{+} \cos\varphi + u_3^{+} \sin\varphi,$$

where R_{b} is the radius of the ring.

Since the problem is symmetric, we will consider the right-hand half of the ring and employ uniform 60×1 finite-element meshes. The calculations were based on the GEX7P4CF and GEX7P4C geometrically exact bilinear shell elements developed with and without account of the follower load. In this case, the assigned calculation accuracy $\varepsilon = 10^{-6}$ according to convergence criterion (34) was achieved. For the regularization parameter, a value optimum for the given class of problems was chosen, namely $\in = 10^2$.

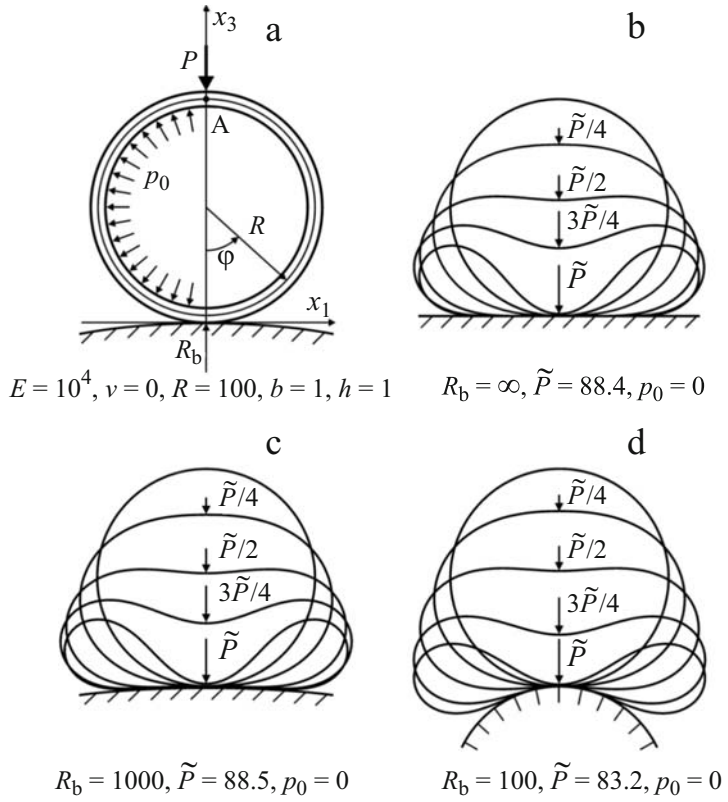

Fig. 2. Scheme of contact interaction of a ring with plane and cylindrical foundations (a) and the deformed structures (b-d).

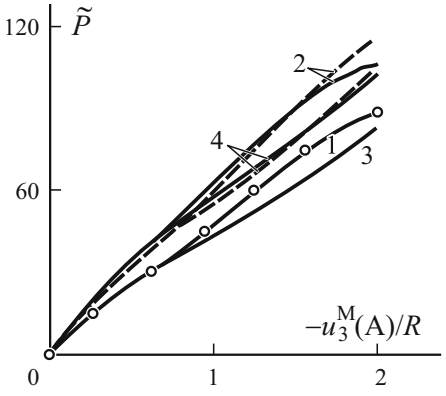

Fig. 3. Load–deflection curves with (——) and without (- - -) account of follower loading for the homogeneous ring: 1 — $R_b = \infty$ and $p_0 = 0$; 2 — $R_b = \infty$ and $p_0 = 10^{-3}$; 3 — $R_b = 100$ and $p_0 = 0$; 4 — $R_b = 100$ and $p_0 = 10^{-3}$.

Figures 2b and 3 show the deformed profiles of the ring and the load–deflection curves for different values of the parameters R_b and p_0. As a nondimensional loading parameter, we assumed $\widetilde{P} = 120PR^2/Eh^3b$. The dots denote the data from [12] obtained by using the classical Timoshenko-type theory of shells. Table 1 presents the transverse displacements u_3^{M} at the

TABLE 1. Comparative Analysis of GEX7P4C and GEX7P4CF Geometrically Exact Shell Elements in the Problem of Contact of a Ring Subjected to a Force $\widetilde{P} = 100$ and Pressure $p_0 = 10^{-3}$ with a Rigid Cylinder of Radius $R_b = 100$, where $D_1 = \{0\} \cup [5\varphi_0, 6\varphi_0]$, $D_2 = [0, 3\varphi_0] \cup \{5\varphi_0\}$, and $\varphi_0 = \pi/60$

Element	Initial contact zone	NLStep	NTStep	NIter	$-u_3^M$(A), mm	$\widetilde{P}_c$	Resulting contact zone
GEX7P4CF	$[0, 5\varphi_0]$	1	6	45	195.3	100.1	D_1
GEX7P4C	$[0, 5\varphi_0]$	1	2	13	192.1	100.1	D_2
GEX7P4CF	$\{0\}$	3	19	100	195.3	100.1	D_1
GEX7P4C	$\{0\}$	3	14	90	192.1	100.1	D_2
GEX7P4CF	$\{0\}$	10	35	119	195.3	100.1	D_1
GEX7P4C	$\{0\}$	10	32	110	192.1	100.1	D_2

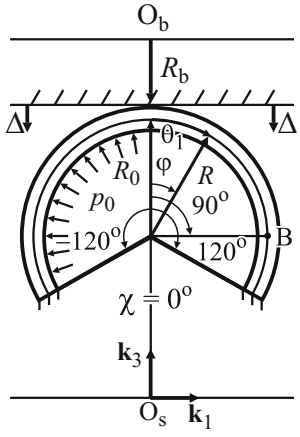

Fig. 4. Contact interaction of a cross-ply toroidal shell with plane ($R_b = \infty$) and cylindrical foundations.

point A and the resulting nodal contact forces $\widetilde{P}_c = 120 P_c R^2 / E h^3 b$ for different numbers of loading steps, NLStep, as well as the total number of steps in the search algorithm of the trial-and-error method, NTStep, and the total number of iterations, NIter, necessary for achieving the calculation accuracy assigned. We should note that, in the case of a successful choice of contact zone, the solution to the problem is possible *without employment* of the incremental approach, i.e., NLStep = 1. In addition, the number of loading steps does not affect the calculated values of displacements and contact forces, which indicates that the geometrically exact shell elements constructed are efficient.

Let us consider now a four-layer cross-ply rubber-cord toroidal shell of circular cross section loaded with a pressure $p_0 = 0.5$ MPa uniformly distributed over its inner surface and compressed by the plane or cylindrical foundation by displacing the latter by Δ in such a way that the clamped sections of the shell with coordinates ±120° remain motionless (Fig. 4). Using this shell, we will model the carcass casing of a diagonal tire. The initial characteristics of elementary rubber-cord layers are as follows [9]: $E_L = 510.45$ MPa, $E_T = 6.91$ MPa, $G_{LT} = 2.33$ MPa, $G_{TT} = 1.77$ MPa, and $\nu_{LT} = 0.46$. Let the shell thickness be $h =$ 4.8 mm, the thickness of a rubber-cord layer $h_k = 1.2$ mm, and the orientations of rubber-cord layers $\gamma_k = (-1)^{k-1}\gamma$, where $\gamma =$ 45° and $k = \overline{1, 4}$. As a reference surface, we assume the shell midsurface formed by rotation of a part of the circumference of ra-

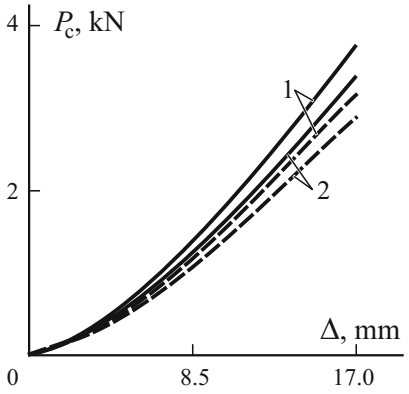

Fig. 5. Load–deflection curves P_c–Δ with (——) and without (- - -) account of follower loading for the cross-ply toroidal shell at $R_b = \infty$ (1) and 1000 mm (2).

TABLE 2. Comparative Analysis of GEX7P4C and GEX7P4CF Geometrically Exact Shell Elements in the Problem of Contact of a Toroidal Shell with the Plane Foundation at $\Delta = 17$ mm, where $D = \{(\varphi, \chi):(5\varphi/\pi)^2 + (10\chi/\pi)^2 \le 1\}$

Element	Initial contact zone	NLStep	NTStep	NIter	u_3^M(B), mm	P_c, N	Area of the contact zone, mm^2
GEX7P4CF	D	1	3	15	3.040	3754	6937
GEX7P4C	D	1	4	20	3.158	3186	6265
GEX7P4CF	(0, 0)	1	8	36	3.040	3754	6937
GEX7P4C	(0, 0)	1	8	36	3.158	3186	6265
GEX7P4CF	(0, 0)	10	33	129	3.040	3754	6937
GEX7P4C	(0, 0)	10	32	125	3.158	3186	6265

dius $R = 50$ mm. The distance from the rotation axis to the equator of midsurface $R_0 = 250$ mm. The nonpenetration conditions for the contacting bodies in the cases of plane and cylindrical foundations are

$$\Psi = R_0 + \frac{1}{2}h - \Delta - \overline{R}_3^+ \ge 0,$$

$$\overline{R}_3^+ = A_2 \cos\chi - u_1^+ \sin\varphi\cos\chi - u_2^+ \sin\chi + \left(\frac{1}{2}h + u_3^+\right)\cos\varphi\cos\chi$$

and

$$\Psi = \frac{1}{2R_b}(\overline{R}_2^+)^2 + \frac{1}{2R_b}\left(R_0 + \frac{1}{2}h + R_b - \Delta - \overline{R}_3^+\right)^2 - \frac{1}{2}R_b \ge 0,$$

$$\overline{R}_2^+ = A_2 \sin\chi - u_1^+ \sin\varphi\sin\chi + u_2^+ \cos\chi + \left(\frac{1}{2}h + u_3^+\right)\cos\varphi\sin\chi,$$

where χ is the circumferential coordinate and $A_2 = R_0 - R(1-\cos\varphi)$ is the Lamé parameter.

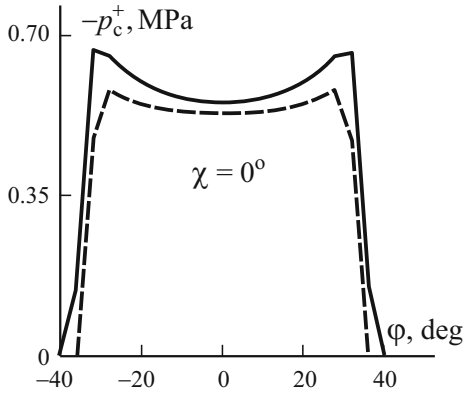

Fig. 6. Distribution of contact pressure in the cases with (——) and without (- - -) account of follower loading for the cross-ply toroidal shell.

Calculation results for the tire under the action of follower and conservative loads were obtained with the help of irregular 48 × 36 finite-element meshes at $\varepsilon = 10^{-6}$ and $\in = 10^4$ (Fig. 5 and Table 2). As is seen, the data in Tables 1 and 2 qualitatively agree with each other. In particular, the solution to this problem for a diagonal tire can also be found without the use of incremental approach. However, the influence of the follower pressure here is displayed to a greater degree. For example, the calculation error for the resultant of nodal contact forces P_c makes 17.8%. In addition, Fig. 6 shows the relation between the contact pressure p_c^+ and the meridional coordinate φ in the central cross section of the shell at $R_b = 1000$ mm and $\Delta = 17$ mm. The results obtained are confirmed by the experimental data presented in [13], namely that the maximum values of contact pressure in a pneumatic tire are shifted toward the boundary of contact area.

This study was financially supported by the Russian Fund for Basic Research (Project No. 08-01-00373) and the Ministry of Education of Russian Federation (Project No. 2.1.1/660).

REFERENCES

1. E. Stein, W. Wagner, and P. Wriggers, "Finite element postbuckling analysis of shells with non-linear contact constraints," in: P. G. Bergan, K. J. Bathe, and W. Wunderlich (eds.), Finite Element Methods for Non-linear Problems, Springer, Berlin (1986), pp. 719-744.
2. Z. H. Zhong, Finite Element Procedures for Contact-Impact Problems, Oxford University Press Inc., Oxford (1993).
3. L. Karaoglan and A. K. Noor, "Sensitivity analysis of frictional contact response of axisymmetric composite structures," Comput. Struct., **55**, No. 6, 937-954 (1995).
4. G. M. Kulikov and S. V. Plotnikova, "Contact problem for a geometrically nonlinear shell of Timoshenko type," Prikl. Matem. Mekh., **67**, No. 6, 940-953 (2003).
5. E. I. Grigolyuk, G. M. Kulikov, and S. V. Plotnikova, "Contact problem for a pneumatic tire interacting with a rigid foundation," Mech. Compos. Mater., **40**, No. 5, 427-437 (2004).
6. G. M. Kulikov and S. V. Plotnikova, "Non-linear strain–displacement equations exactly representing large rigid-body motions. Pt. III. Analysis of TM shells with constraints," Comput. Meth. Appl. Mech. Eng., **196**, No. 7, 1203-1215 (2007).
7. J. C. Simo, P. Wriggers, and R. L. Taylor, "A perturbed Lagrangian formulation for the finite element solution of contact problems," Comput. Meth. Appl. Mech. Eng., **50**, No. 2, 163-180 (1985).

8. G. M. Kulikov and S. V. Plotnikova, “Finite rotation geometrically exact four-node solid-shell element with seven displacement degrees of freedom,” Comput. Model. Eng. Sci., **28**, No. 1, 15-38 (2008).
9. G. M. Kulikov and S. V. Plotnikova, “Calculation of composite structures subjected to follower loads by using a geometrically exact shell element,” Mech. Compos. Mater., **45**, No. 6, 545-556 (2009).
10. A. S. Sakharov and I. Altenbach (eds.), Finite-Element Method in Mechanics of Solid Bodies [in Russian], Vishcha Shkola, Kiev (1982).
11. K. J. Bathe, Finite Element Procedures, Prentice Hall, New York (1996).
12. A. K. Noor and K. O. Kim, “Mixed finite element formulation for frictionless contact problems,” Finite Elem. Anal. Des., **4**, No. 4, 315-332 (1989).
13. R. A. Ridha and M. Theves, “Advances in tire mechanics,” in: IRC 94. Vol. 1, Moscow (1994), pp. 54-126.